The action mechanism by which C1q/tumor necrosis factor-related protein-6 alleviates cerebral ischemia/reperfusion injury in diabetic mice

Bo Zhao[1, #], Mei Li[1, #], Bingyu Li[1, #], Yanan Li[1], Qianni Shen[1], Jiabao Hou[1], Yang Wu[1], Lijuan Gu[2, *], Wenwei Gao[3, *]

https://doi.org/10.4103/1673-5374.390951

Date of submission: August 17, 2022

Date of decision: December 28, 2022

Date of acceptance: July 29, 2023

Date of web publication: December 15, 2023

From the Contents

Graphical Abstract

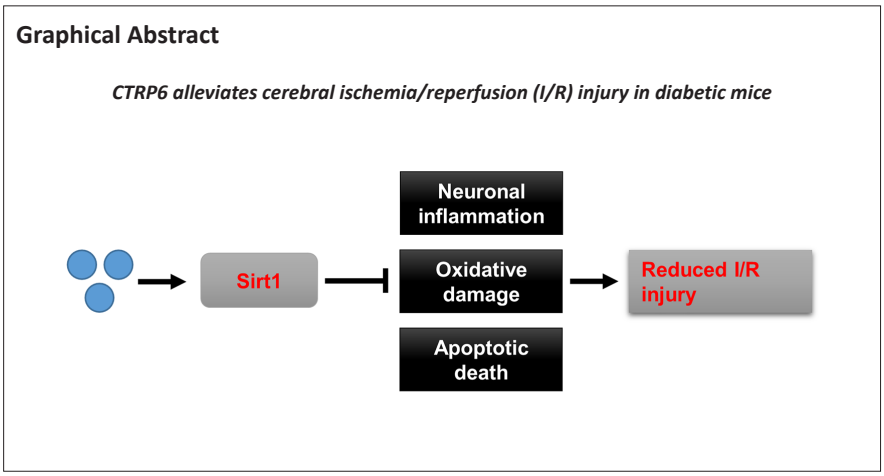

Abstract

Studies have shown that C1q/tumor necrosis factor-related protein-6 (CTRP6) can alleviate renal ischemia/reperfusion injury in mice. However, its role in the brain remains poorly understood. To investigate the role of CTRP6 in cerebral ischemia/reperfusion injury associated with diabetes mellitus, a diabetes mellitus mouse model of cerebral ischemia/reperfusion injury was established by occlusion of the middle cerebral artery. To overexpress CTRP6 in the brain, an adeno-associated virus carrying CTRP6 was injected into the lateral ventricle. The result was that oxygen injury and inflammation in brain tissue were clearly attenuated, and the number of neurons was greatly reduced. *In vitro* experiments showed that CTRP6 knockout exacerbated oxidative damage, inflammatory reaction, and apoptosis in cerebral cortical neurons in high glucose hypoxia-simulated diabetic cerebral ischemia/reperfusion injury. CTRP6 overexpression enhanced the sirtuin-1 signaling pathway in diabetic brains after ischemia/reperfusion injury. To investigate the mechanism underlying these effects, we examined mice with depletion of brain tissue-specific sirtuin-1. CTRP6-like protection was achieved by activating the sirtuin-1 signaling pathway. Taken together, these results indicate that CTRP6 likely attenuates cerebral ischemia/reperfusion injury through activation of the sirtuin-1 signaling pathway.

Key Words: brain; C1q/tumor necrosis factor-related protein-6; cerebral apoptosis; diabetes; inflammation; ischemia/reperfusion injury; neuron; neuroprotection; oxidative damage; Sirt1

Introduction

Patients with diabetes are vulnerable to stroke because diabetes can increase the fragility of brain vessels and induce neuronal apoptosis (Desilles et al., 2013; Alloubani et al., 2018; Fang et al., 2022). Numerous studies have reported effective approaches to treat ischemic stroke, but only thrombolytic therapy has been proven to be successful in clinical practice (Capes et al., 2001). Unfortunately, this classic treatment has been reported to increase the risk of cerebral hemorrhage and worsen the clinical outcome of these patients (Capes et al., 2001). Although other therapies can improve functional recovery in response to ischemic injury, they can also have adverse side events, such as cerebral arteriosclerosis-like changes (Chen et al., 2011; Liu et al., 2021). Novel effective neuroprotectants are urgently needed to reduce the risk of ischemia/reperfusion (I/R)-related brain injury in patients with diabetes.

The pathogenesis of cerebral I/R injury is complex, but accumulative data have demonstrated that oxidative damage, inflammation, and apoptosis play critical roles in the process (Pacher and Haskó, 2008; Stoll and Nieswandt, 2019; Qiu et al., 2023; Ugidos et al., 2023). For example, excessive production of free radicals was observed in diabetic stroke (Forrester et al., 2018), and Moro et al. (2005) reported that reactive oxygen species (ROS) produced after exposure to I/R cause lipid peroxidation and protein denaturation, eventually resulting in brain damage. ROS directly induce nuclear factor kappa B (NF-κB) activation, triggering a myriad of pro-inflammatory responses in mice with cerebral I/R injury (Morgan and Liu, 2011). Additionally, ROS production and inflammation accumulation induce the onset of neuronal apoptosis, which is an important pathological mediator of ischemic stroke (Morgan and Liu, 2011). Therefore, effective neuroprotectants that selectively suppress these pathological processes are being sought for their potential to prevent diabetic stroke.

C1q/tumor necrosis factor-related protein 6 (CTRP6) has been reported to protect against cardio-metabolic diseases and cancer (Lei et al., 2017; Wang et al., 2018a). Specifically, CTRP6 attenuates doxorubicin-induced cardiac damage via protein kinase B activation (Zheng et al., 2019). In obese mice, its expression was also found to be elevated and it affected the expression of inflammatory factors produced by adipose tissues (Lei et al., 2017; Wu et al., 2018). Xiang et al. (2020) reported that CTRP6 attenuated renal I/R injury by reducing oxidative injury in mice. However, the CTRP6 in the brain has not been further explored, especially in individuals with diabetes mellitus. Therefore, the present work was designed to investigate whether CTRP6 can inhibit cerebral I/R injury in a mouse model of diabetes mellitus, and if so, to determine the molecular basis.

Methods

Animals

Male C57BL/6 mice (age 9–10 weeks; body weight 23 ± 2 g) were provided by Beijing Vital River Laboratory Animal Technology Co., Ltd. (license No.

[1]Department of Anesthesiology, Renmin Hospital of Wuhan University, Wuhan, Hubei Province, China; [2]Central Laboratory, Renmin Hospital of Wuhan University, Wuhan, Hubei Province, China; [3]Department of Critical Care Medicine, Renmin Hospital of Wuhan University, Wuhan, Hubei Province, China

*Correspondence to: Wenwei Gao, MD, gaowenwei@whu.edu.cn; Lijuan Gu, MD, PhD, gulijuan@whu.edu.cn.

https://orcid.org/0000-0003-4405-0168 (Wenwei Gao); https://orcid.org/0000-0003-1928-8772 (Lijuan Gu)

*These authors contributed equally to this work.

Funding: *This study was supported by the National Natural Science Foundation of China, Nos. 82102295 (to WG), 82071339 (to LG), 82001119 (to JH) and 81901994 (to BZ).*

How to cite this article: *Zhao B, Li M, Li B, Li Y, Shen Q, Hou J, Wu Y, Gu L, Gao W (2024) The action mechanism by which C1q/tumor necrosis factor-related protein-6 alleviates cerebral ischemia/reperfusion injury in diabetic mice. Neural Regen Res 19(9):2019-2026.*

SYXK [Jing] 2021-0080, Beijing, China), and were kept in our animal center at a standard temperature (23 ± 2°C) and humidity (50–60%) under a 12/12-hour light/dark period. Four mice were kept per cage to allow free activity. The study was approved by the Medical Faculty Ethics Committee of Renmin Hospital of Wuhan University (No. WDRM20210807D, approval date: August 31, 2021). All experiments were designed and reported according to the ARRIVE (Animal Research: Reporting of *In Vivo* Experiments) guidelines (Percie du Sert et al., 2020).

We used streptozotocin (STZ, CAS# 18883-66-4, Sigma-Aldrich, St. Louis, MO, USA) to induce diabetes mellitus in mice. Mice were fasted overnight and subjected to intraperitoneal injections of 50 mg/kg STZ for 5 consecutive days, as previously described (Liu et al., 2021). After 5 days, mice with fasting blood-glucose levels greater than 13.9 mM in three independent measurements were judged to have diabetes mellitus (Ma et al., 2017). Six weeks after they developed diabetes, the I/R model was generated by transient middle cerebral artery occlusion (tMCAO) (Wang et al., 2012). Briefly, mice were anesthetized with inhaled isoflurane (2.5%, Sigma-Aldrich, Cat# 26675-46-7) (Wang et al., 2013) and transient ischemia was induced by tMCAO, as described previously (Gu et al., 2012; Xiong et al., 2014). In brief, the origin of the middle cerebral artery was exposed and occluded using a monofilament surgical suture. After 60 minutes, the filament was withdrawn. In a control sham group of mice, the procedure was similar, but without ligation. To detect CTRP6 expression during I/R, the brain samples were collected at 0.5, 2, 6, 12, 24, 48 or 72 hours after reperfusion onset. To investigate the role of CTRP6 in diabetic stroke, the diabetic mice were randomly divided into three groups: Sham, I/R, and I/R + CTRP6. To overexpress cerebral CTRP6, mice were given an intracerebroventricular injection of adeno-associated virus-2/9 (AAV-2/9) carrying human CTRP6 under the calcium/calmodulin-dependent protein kinase II (CaMKII) alpha promoter (AAV-CTRP6, 7.18×10^{12} viral genome/mouse; Hanbio, Shanghai, China) 3 weeks post STZ injection (Gray et al., 2010; Liu et al., 2015). Mice in the Sham and I/R groups received an injection of AAV-2/9 carrying a negative control (NC) under the CaMKII alpha promoter (Hanbio). We confirmed that CTRP6 was overexpressed 3 weeks after injection by performing western blot assays in mice that were euthanized with 200 mg/kg sodium pentobarbital (Sigma-Aldrich). Therefore, for the experimental mice, we performed the I/R model surgeries at this time point.

Results from the CTRP6-protection analyses led us to hypothesize that CTRP6-mediated protection from stroke in our mouse model of diabetes mellitus was dependent on sirtuin-1 (Sirt1) activation. To test this hypothesis, we depleted Sirt1 in the brain by breeding Sirt1 flox mice (B6.129-Sirt1^{tm3Fwa}/DsinJ, Jackson, Bar Harbor, ME, USA, strain # 029603, RRID: IMSR_JAX:029603) with CaMKII alpha-Cre transgenic mice to generate mice with brain-specific Sirt1 depletion. Tamoxifen (80 mg/kg, Sigma-Aldrich) was intraperitoneally injected for 5 consecutive days to achieve the brain-specific Sirt1 depletion. These conditional Sirt1-depletion mice also received an intracerebroventricular injection of AAV-CTRP6 or AAV-NC and tMCAO surgery (Liu et al., 2015).

Neurological deficit scores and water content assessment

At 1 or 3 days after tMCAO, we evaluated neurological deficits and brain water content, as previously described (Liu et al., 2021). Neurological deficits were evaluated on a nine-point scale by researchers blinded to the mouse groupings. Water content of the brain was calculated using the following formula: brain water content (%) = 100 × (wet weight – dry weight)/wet weight

Cerebral infarct volume measurement

During tMCAO, we used a laser Doppler flow meter (Perimed, Stockholm, Sweden) for continuous monitoring of the cerebral blood flow (CBF). Greater than 80% decline in relative CBF confirmed a CBF interruption (Liu et al., 2015). At 1 or 3 days after tMCAO, the brains were immediately collected and sectioned (2 mm/section) after anesthesia. The sections were reacted with 2% 2,3,5-triphenyl tetrazolium chloride (TTC, Sigma-Aldrich, CAS# 298-96-4) for 30 minutes and fixed in a formalin solution (10%). The brain sections were then observed under a camera and evaluated with ImageJ software (version 1.8.0; National Institutes of Health, Bethesda, MD, USA; Wang et al., 2012; Liu et al., 2021). Cerebral infarct volume was analyzed by one author who was unaware of the animal groupings.

Western blotting

One day after reperfusion, the brain samples were lysed in a radio immunoprecipitation assay lysis buffer. After separation via 10% sodium dodecyl sulfate-polyacrylamide gel electrophoresis (SDS-PAGE), proteins were transferred to polyvinylidene difluoride membranes (Millipore, Billerica, MA, USA). The membranes were incubated with CTRP6 (rabbit polyclonal, 1:500, Abcam, Cambridge, UK, Cat# ab36898, RRID: AB_731489), glyceraldehyde-3-phosphate dehydrogenase (GAPDH; mouse monoclonal, 1:5000, Abcam, Cat# ab8245, RRID: AB_2107448), nuclear factor (erythroid-2 related) factor 2 (Nrf2; rabbit monoclonal, 1:1000, Abcam, Cat# ab62352, RRID: AB_944418), NF-κB (rabbit polyclonal, 1:1000, Abcam, Cat# ab16502, RRID: AB_443394), phosphorylated-NF-κB (P-NF-κB; rabbit monoclonal, 1:1000, Abcam, Cat# ab76302, RRID: AB_1524028), heme oxygenase 1 (HO-1; rabbit monoclonal, 1:1000, Abcam, Cat# ab52947, RRID: AB_880536), NAD(P)H quinone oxidoreductase-1 (NQO-1; rabbit monoclonal, 1:1000, Abcam, Cat# ab80588, RRID: AB_1603750), superoxide dismutase (SOD-1; rabbit monoclonal, 1:2000, Abcam, Cat# ab51254, RRID: AB_882757), catalase (CAT; rabbit monoclonal, 1:1000, Abcam, Cat# ab209211), phosphorylated-IκB kinase α (P-IKKα; rabbit polyclonal, 1:1000, Abcam, Cat# ab38515, RRID: AB_881450), IKKα (rabbit monoclonal, 1:1000, Abcam, Cat# ab32041, RRID: AB_733070), inhibitor of nuclear factor kappa-B kinase (IκBα; rabbit monoclonal, 1:1000, Cell Signaling Technology, Beverly, MA, USA, Cat# 9242, RRID: AB_331623), phosphorylated-IκBα (P-IκBα; rabbit monoclonal, 1:1000, Cell Signaling Technology, Cat# 2859), Bcl-2 (rabbit monoclonal, 1: 500, Abcam, Cat# ab182858, RRID: AB_2715467), Bax (rabbit monoclonal, 1:400, Abcam, Cat# ab32503, RRID: AB_725631), Sirt1 (mouse monoclonal, 1:1000, Abcam, Cat# ab110304, RRID: AB_10864359), and proliferating cell nuclear antigen (PCNA; mouse monoclonal, 1:1000, Abcam, Cat# ab29, RRID: AB_303394) overnight at 4°C. Subsequently, the polyvinylidene difluoride membranes were incubated with goat anti-rabbit IgG (H+L) cross-adsorbed secondary antibody, HRP (1:10,000, Thermo Fisher Scientific, Waltham, MA, USA, Cat# G-21234, RRID: AB_2536530) or goat anti-mouse IgG (H+L) cross-adsorbed secondary antibody (1:10,000, Thermo Fisher Scientific, Cat# 31164, RRID: AB_228299) at 37°C for 2 hours and enhanced chemiluminescence reagent (Thermo Fisher Scientific, Cat# WP20005). GAPDH was used as the endogenous control and the blots were quantified by ImageJ.

Real-time polymerase chain reaction

We extracted total RNA from the brains one day after reperfusion using TRIzol reagent (Invitrogen, Carlsbad, CA, USA), and 2 μg of the total RNA was reverse-transcribed by the OneStep Ahead RT-PCR Kit (Qiagen, Berlin, Germany). Real-time PCR was performed using a SYBR Green Master Mix kit (Roche, Basel, Switzerland). The primer sequences are shown in **Table 1**. All samples were run in triplicate, and GAPDH was used as the endogenous control.

Table 1 | **Primer sequences for real-time polymerase chain reaction**

Primer	Sequence
Gapdh	Forward: 5'-ACT CCA CTC ACG GCA AAT TC-3'
	Reverse: 5'-TCT CCA TGG TGG TGA AGA CA-3'
Ctrp6	Forward: 5'-ATC ACA GAC ATG GGC CAA GG-3'
	Reverse: 5'-TCA ACT CAC AGA CCC CGG AC-3'
Nrf2	Forward: 5'-GTG GTT TAG GGC AGA AGG-3'
	Reverse: 5'-TCT TTC TTA CTC TGC CTC TA-3'
Hmox1	Forward: 5'-GAC AGA AGA GGC TAA GAC CGC-3'
	Reverse: 5'-TGA CGA AGT GAC GCC ATC T-3'
Nqo1	Forward: 5'-GCG AGA AGA GCC CTG ATT GT-3'
	Reverse: 5'-CTT CAG CTC ACC TGT GAT GTC AT-3'
Cat	Forward: 5'-CCT ATT GCC GTT CGA TTC TC-3'
	Reverse: 5'-CCC ACA AGA TCC CAG TTA CC-3'
Gpx3	Forward: 5'-CAG TTC GGA CAT CAG GAG AAT-3'
	Reverse: 5'-AGA GCG GGT GAG CCT TCT-3'
Sod1	Forward: 5'-GCA TTC CAT CAT TGG CCG TA-3'
	Reverse: 5'-TTT CCA CCT TTG CCC AAG TCA-3'
Sod2	Forward: 5'-GTG TCT GTG GGA GTC CAA GG-3'
	Reverse: 5'-CCC CAG TCA TAG TGC TGC AA-3'
Tnf-α	Forward: 5'-CCC TCA CAC TCA CAA ACC ACC-3'
	Reverse: 5'-CTT TGA GAT CCA TGC CGT TG-3'
Mcp-1	Forward: 5'-CGC ACT AGG TTT GCC GAG TA-3'
	Reverse: 5'-TGT CTG GAC CCA TTC CTT CTT G-3'
Il-1β	Forward: 5'-TCA TTG TGG CTG TGG AGA AG-3'
	Reverse: 5'-AGG CCA CAG GTA TTT TGT CG-3'
Il-2	Forward: 5'-TCT ACA GCG GAA GCA CAG CA-3'
	Reverse: 5'-AAT CCA GAA CAT GCC GCA GA-3'
Il-6	Forward: 5'-AGG AGA AAG ACC ATT ACT GTA TCA C-3'
	Reverse: 5'-TGA GGA ATG TCC ACA AAC TGA TA-3'
Vcam-1	Forward: 5'-GAT ACA ACC GTC TTG GTC AGC CC-3'
	Reverse: 5'-CGC ATC CTT CAA CTG GGC CTT-3'
Cox2	Forward: 5'-GCA GCC AGT TGT CAA ACT GC-3'
	Reverse: 5'-CTC GGA GAG CAT CGC AGA GG-3'
Ifng	Forward: 5'-ATC TGG AGG AAC TGG CAA AA-3'
	Reverse: 5'-TTC AAG ACT TCA AAG AGT CTG AGG TA-3'
Il-17	Forward: 5'-TCT CAT CCA GCA AGA GAT CC-3'
	Reverse: 5'-AGT TTG GGA CCC CTT TAC AC-3'
Il-4	Forward: 5'-CAT CGG CAT TTT GAA CGA G-3'
	Reverse: 5'-CGA GCT CAC TCT CTG TGG TG-3'

Oxidative damage assay and inflammatory factor detection

Cerebral oxidative damage in the brain after 24-hour tMCAO was assessed by quantifying glutathione (GSH) and malondialdehyde (MDA) content in the brain, as well as SOD and CAT activity. Kits for detecting GSH content (Cat# A006-2-1), MDA content (Cat# A003-1-2), total SOD activity (Cat# A001-3-2), and CAT activity (Cat# A007-1-1) were provided by Nanjing Jiancheng Bioengineering Institute (Nanjing, Jiangsu, China). A 4-hydroxynonenal (4-HNE) assay kit (E4645-100, Biovision, San Francisco, CA, USA) was used to detect 4-HNE levels in the brain.

To detect inflammatory factors, fresh brain samples from mice after 24-hour I/R were homogenized in normal saline. Tumor necrosis factor-α (TNF-α), interleukin-1β (IL-1β), and monocyte chemoattractant protein-1 (MCP-1) levels in the brains were detected using commercial kits. Mouse TNF-α uncoated enzyme-linked immunosorbent assay (ELISA) (Cat# 88-7324), IL-1β pro-form mouse uncoated ELISA Kit with plates (Catalog # 88-8014-22), and MCP-1 Mouse ELISA Kit (Cat # BMS6005) were provided by Thermo Fisher (Beverly, MA, USA).

Terminal deoxynucleotidyl transferase dUTP nick-end labeling staining and caspase activity detection

To detect neuronal apoptosis, the brain samples were reacted with an ApopTag Plus In Situ Apoptosis Fluorescein Detection Kit (S7111; Millipore). The sections were observed under a fluorescence microscope (Olympus, Tokyo, Japan). We then used Caspase-3 Activity Assay Kit (Luminometric, #K186-100, Biovision) and Caspase 9 Activity Apoptosis Assay Kit (Cat# E607118, Sangon Biotech, Shanghai, China) to measure caspase 3 and caspase 9 activity.

Cortical neuron culture and treatment

We separated primary cortical neurons from ten neonatal Sprague-Dawley rat brains (1–3 days old, provided by Beijing Vital River Laboratory Animal Technology Co., Ltd.; Lu et al., 2013). In brief, these neonatal rats were sacrificed by cervical dislocation (NIH Office of Animal Care and Use, 2021) and the brains were collected and dissociated in trypsin (0.125%) for 15–20 minutes at 37°C. After being centrifuged for 5 minutes, the cells were then suspended in Dulbecco's modified Eagle medium (Gibco, Rockville, MD, USA) containing 15% fetal bovine serum (Gibco). After that, the separated neurons were grown in Neuro-basal/B27 medium (Thermo Fisher Scientific, Cat# A3653401) for 24 hours. To mimic diabetic status, the cells were incubated with a high-glucose (50 mM) medium for 8 hours before hypoxia/reoxygenation (H/R) stimulation and throughout the entire experimental period (Liu et al., 2021). Next, the cells were subjected to 6-hour hypoxic incubation to generate H/R injury, followed by normal culture conditions for various lengths of time. To investigate the effect of CTRP6 during H/R, these cells were divided into control, H/R, and H/R + CTRP6 groups. The cells were pretreated with the recombinant full-length CTRP6 protein (8 μg/mL, Aviscera Bioscience, Santa Clara, CA, USA) for 12 hours and then exposed to H/R treatment (Zheng et al., 2019b). To further investigate the protective role of CTRP6, we used an adenoviral vector (Ad) system to overexpress human CTRP6. Briefly, neurons were treated with Ad-*CTRP6* (Hanbio) diluted in medium with a multiplicity of infection (MOI) of 75. After 4-hour infection, cells were subjected to high-glucose medium for 8 hours before H/R treatment. To knock down Ctrp6, cells were subjected to the adenoviral vectors carrying CTRP6 small hairpin RNAs (sh*Ctrp6*, Hanbio, MOI = 150) or shRna (Hanbio, MOI = 150) for 4 hours. The cells were then pre-incubated with Ex527 (a specific inhibitor of Sirt1, 1 μM, MedChemExpress, Monmouth Junction, NJ, USA) 6 hours before H/R treatment. To assess Nrf2 transactivation after CTRP6 treatment, the CTRP6-overexpressing cells were electro-transfected with Nrf2-luc (0.03 μg) using the Neon® Transfection System (Thermo Fisher Scientific). To evaluate NF-κB suppression, the CTRP6-overexpressing cells were electro-transfected with NF-κB-luc (0.03 μg, Yeasen, Shanghai, China).

Reactive oxygen species detection

The cortical neurons were grown in a 96-well plate, pretreated with a high-glucose medium, and then exposed to H/R stimuli. Next, the neurons were treated with 2,7-dichlorofluorescin diacetate (DCFH-DA, 10 μM, Nanjing Jiancheng Bioengineering Institute) for 3 ho urs at 37°C, and intensity of the fluorescence was determined by a microplate reader (BioTek, Winooski, VT, USA) (Ma et al., 2016).

Analysis of cell viability and cell injury

Viability of neurons was determined by counting the number of cells using a cell-counting kit-8 kit (Dojindo, Kumamoto, Japan). To further evaluate cell injury after H/R, lactate dehydrogenase (LDH) release was also detected using a microplate reader (BioTek).

Statistical analysis

The necessary sample numbers for the animal experiments were estimated by holding the probability of a type I error at $\alpha = 0.05$. In our study, animal numbers in each group clearly fulfilled the requirement. The data are presented as the mean ± standard error of the mean (SEM). The Shapiro-Wilk test was used to evaluate data normality. An unpaired two-sided Student's *t*-test was used to compare the differences between two groups. One-way analysis of variance was used to compare the differences among multiple groups, followed by a *post hoc* Tukey's test. Statistical analyses were carried out using SPSS 22.0 software (IBM, Armonk, NY, USA). A level of $P < 0.05$ was considered statistically significant.

Results

CTRP6 expression is lower than controls in diabetic mice after cerebral I/R injury

The distribution of *Ctrp6* mRNA in non-diabetic mouse organs was detected by real-time PCR, and Ctrp6 mRNA was highly expressed in the brain and adipose tissues of non-diabetic mice, with the most abundant Ctrp6 mRNA in the brain (**Figure 1A**). Next, levels of CTRP6 expression after I/R were determined in diabetic mice. Analysis showed that compared with non-diabetic mice, levels of Ctrp6 mRNA in the brains of I/R-exposed diabetic mice were time-dependently downregulated (**Figure 1B** and **C**). In response to 24-hour I/R, cerebral CTRP6 expression was also downregulated in these diabetic mice (**Figure 1D**). The downregulation of CTRP6 expression was also observed in H/R-treated neurons (**Figure 1E** and **F**). These data indicate that CTRP6 reduction is involved in the development of ischemic stroke in diabetic mice.

CTRP6 loss of function induces pro-inflammatory factor production, oxidative stress, and neuron death in the model of cerebral I/R injury

In light of the decreased CTRP6 observed in H/R-treated cortical neurons, we silenced *Ctrp6* expression in neurons. Surprisingly, downregulation of CTRP6 protein increased cellular ROS and lipid peroxidation products in high glucose-treated cells, even without H/R stimuli (**Figure 2A–C**). *Ctrp6* deficiency also decreased Nrf2 protein expression and its transcriptional activity in high glucose-treated cells, even without H/R stimuli (**Figure 2D** and **E**). Further analysis revealed that levels of mRNA for antioxidant enzymes *Nrf2*, *Hmox1*, *Nqo1*, and *Cat* were all downregulated in *Ctrp6*-deficient cortical neurons, even without H/R stimuli (**Figure 2F**). The results also showed that *Ctrp6* depletion in cortical neurons caused increased phosphorylation of NF-κB (**Figure 2G**). Downregulation of *Ctrp6* increased NF-κB transcriptional activity and NF-κB-regulated gene expression in high glucose-treated cells, even without H/R stimuli (**Figure 2H** and **I**). In high-glucose alone conditions, CTRP6 depletion caused death of more neurons and increased LDH release in a time-dependent manner (**Figure 2J** and **K**).

CTRP6 overexpression reduces cerebral I/R injury in diabetic mice

To overexpress cerebral CTRP6, mice from the I/R + CTRP6 group received an intracerebroventricular injection of AAV-CTRP6 3 weeks post STZ injection. The timeline of experimental procedures is shown in **Figure 3A**. As indicated in **Figure 3B**, the reduced CTRP6 protein expression observed the I/R group was restored in the I/R + CTRP6 group. Next, the brain regions in which the expression of Ctrp6 was elevated were determined. The AAV infection significantly increased cortical *Ctrp6*, and slightly increased thalamus Ctrp6 expression, without affecting *Ctrp6* expression in the hippocampus or midbrain (**Figure 3C**). We next determined that intracerebroventricular injection did not affect blood glucose or body weight in the diabetic mice from any of the three groups (**Figure 3D** and **E**). Additionally, neurological deficit scores were higher in the I/R + CTRP6 group than in the I/R group 24 hours (26% reduction) and 72 hours (45% reduction) after cerebral I/R (**Figure 3F**). More importantly, the cerebral infarct area was smaller in the I/R + CTRP6 group than in the I/R group 24 hours (7.02 ± 0.91 *vs.* 21.22 ± 1.89, $P < 0.05$) and 72 hours (10.01 ± 0.84 *vs.* 23.96 ± 1.55, $P < 0.05$) after ischemic onset (**Figure 3G** and **H**). CTRP6 supplementation also significantly decreased brain edema after cerebral I/R in the mouse model of diabetes mellitus (**Figure 3I**).

CTRP6 overexpression attenuates cerebral oxidative damage, inflammatory reaction, and apoptosis in diabetic mice with cerebral I/R injury

Allen and Bayraktutan (2009) reported that oxidative damage occurred after cerebral I/R. After exposure to 24-hour I/R, diabetic mice exhibited a reduction in GSH content relative to the Sham group, and CTRP6 resulted in higher GSH content after I/R (**Figure 4A**). Treatment with CTRP6 restored the decline in SOD and CAT activity in the brains of diabetic mice with I/R (**Figure 4B** and **C**). CTRP6 also decreased MDA and 4-HNE content in diabetic mice following I/R (**Figure 4D** and **E**). The expression levels of anti-oxidative genes (*Nrf2*, *Hmox1*, *Nqo1*, *Cat*, *Gpx3*, *Sod1* and *Sod2*) were significantly lower following 24-hour I/R than they were in the Sham mice, and these declines were prevented by CTRP6 overexpression (**Figure 4F**). The protein levels of Nrf2, HO-1, NQO-1, and SOD-1 were also upregulated in CTRP6 overexpressed diabetic mice (**Figure 4G**).

Neuroinflammation plays profound roles in diabetic stroke (Lindsberg and Grau, 2003). We detected an inflammatory response in CTRP6-overexpressing diabetic mice. The mRNA of numerous pro-inflammatory factors, such as *Tnf-α*, *Mcp-1*, *Il-1β*, *Il-2*, *Il-6*, *Vcam-1*, *Cox2*, *Ifng*, *Il-17*, and *Il-4* were higher in the I/R group, and these elevations were suppressed by CTRP6 overexpression (**Figure 5A**). However, CTRP6 did not affect the elevated levels of IL-4 that were observed in the I/R group (**Figure 5A**). ELISA confirmed the mRNA results. CTRP6 alleviated the pathological accumulation of IL-1β, TNF-α, and MCP-1 that wasfound in the I/R group (**Figure 5B–D**). As reported, NF-κB regulates several inflammatory genes and plays a key role in cerebral diseases (Wang et al., 2019). CTRP6 supplementation attenuated phosphorylation of IKKβ, IκBα, and NF-κB in the diabetic mice (**Figure 5E**). Next, we found that apoptosis-related proteins were also affected by CTRP6 treatment. CTRP6 supplementation increased Bcl-2 and decreased Bax in diabetic mice after I/R (**Figure 5F**). Consistent with these findings, we also observed that CTRP6 overexpression decreased the elevated caspase 3 and caspase 9 activity that was observed in diabetic brains after I/R (**Figure 5G** and **H**). Terminal deoxynucleotidyl transferase-mediated dUTP nick end labeling (TUNEL) staining showed that CTRP6 overexpression significantly reduced the number of TUNEL-positive cells in diabetic brains after I/R (**Figure 5I**).

CTRP6 protects neurons *in vitro* from H/R-induction

To determine the direct impact of CTRP6 *in vitro*, cultured cortical neurons were treated with the recombinant CTRP6 protein. Without H/R stimulation, no differences among the three groups were observed in neuronal survival and LDH release (**Figure 6A** and **B**). However, when challenged with H/R, CTRP6 treatment reduced both the number of damaged neurons and the amount of LDH that the neurons released (**Figure 6A** and **B**). Neurons were also made to overexpress CTRP6 via adenoviral infection. CTRP6 overexpression suppressed H/R-induced cell loss and LDH release (**Figure 6C–E**). *Nrf2*, *Hmox1*,

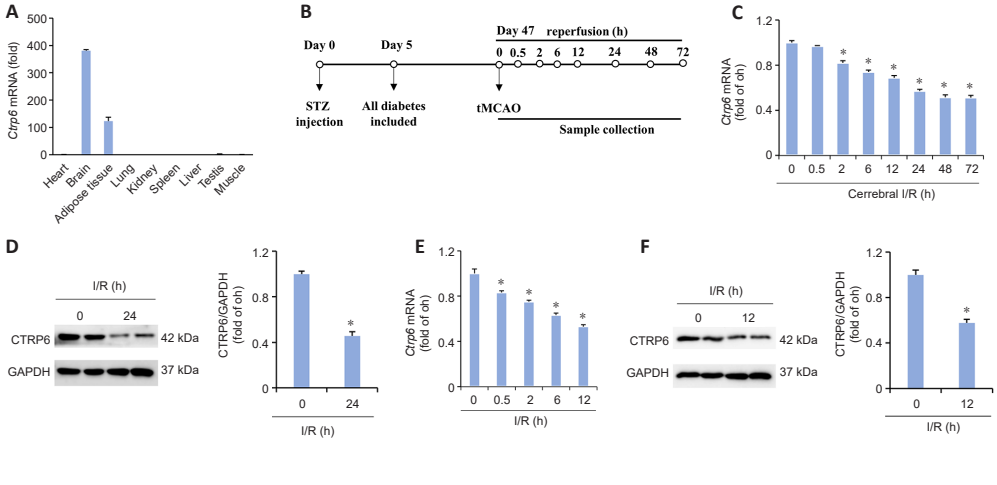

Figure 1 | C1q/tumor necrosis factor-related protein-6 (CTRP6) expression in the brain is suppressed by ischemia/reperfusion (I/R) injury.
(A) *Ctrp6* mRNA level in several organs of non-diabetic mice by real-time polymerase chain reaction (four or five animals per group). (B) The timeline of experimental procedures. (C) *Ctrp6* mRNA level in mice with I/R (five animals for each time point). (D) Western blotting revealed that CTRP6 protein expression was reduced after ischemia (six animals per group). (E) *Ctrp6* mRNA level in cultured cortical neurons with hypoxia/reoxygenation (H/R) (five independent cell culture preparations for each time point). (F) CTRP6 protein expression was detected in cultured cortical neurons with H/R (six independent cell culture preparations per group). The results are presented as the mean ± SEM, and were analyzed by unpaired two-sided Student's *t*-test (D and F) or one-way analysis of variance followed by *post hoc* Tukey's test (C and E). *$P < 0.05$, *vs.* I/R (0 hour) or H/R (0 hour) group. For C to F, data were normalized by I/R (0 hour) or H/R (0 hour) group. GAPDH: Glyceraldehyde-3-phosphate dehydrogenase; STZ: streptozotocin; tMCAO: transient middle cerebral artery occlusion.

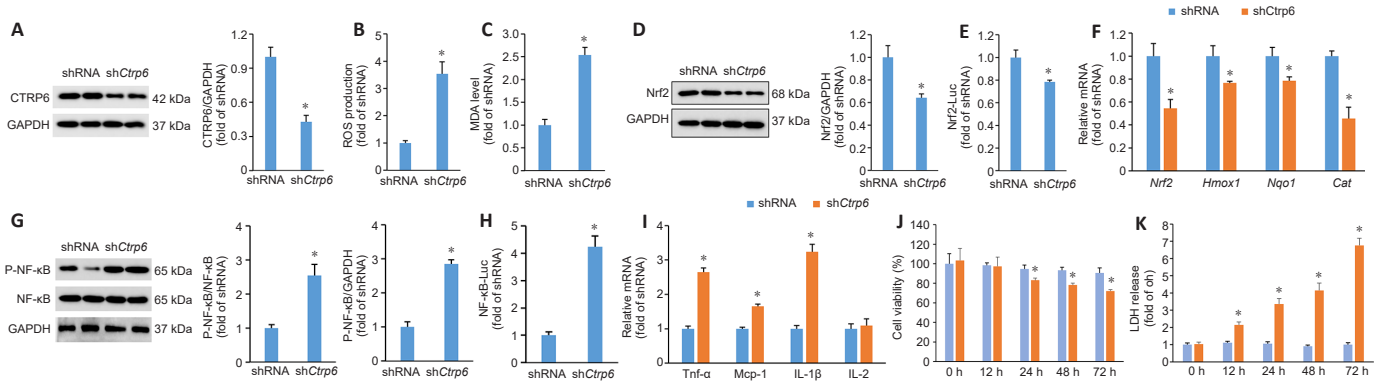

Figure 2 | C1q/tumor necrosis factor-related protein-6 (CTRP6) deficiency causes oxidative damage, inflammation, and cell apoptosis under basal conditions.
(A) CTRP6 protein expression as detected by western blotting. (B, C) The production of reactive oxygen species (ROS) and malondialdehyde (MDA) after *Ctrp6* deficiency *in vitro*. (D, E) Nuclear factor (erythroid-2 related) factor 2 (Nrf2) protein expression and transcriptional activity after *Ctrp6* deficiency *in vitro*. (F) The mRNA levels of *Nrf2*-regulated genes. (G) Phosphorylation of nuclear factor kappa B (NF-κB) *in vitro*. (H, I) NF-κB transcriptional activity and its downstream genes *in vitro*. (J, K) Cell viability and lactate dehydrogenase (LDH) release *in vitro* after *Ctrp6* deficiency. All data were normalized to the shRNA group. For each experiment, five or six independent cortical neuron preparations were used per group. The results are presented as the mean ± SEM, and were analyzed by unpaired two-sided Student's *t*-test. *$P < 0.05$, *vs.* shRna group. GAPDH: Glyceraldehyde-3-phosphate dehydrogenase; IL: interleukin; Mcp-1: monocyte chemoattractant protein-1; P-NF-κB: phosphorylated-NF-κB; Tnf-α: tumor necrosis factor-α.

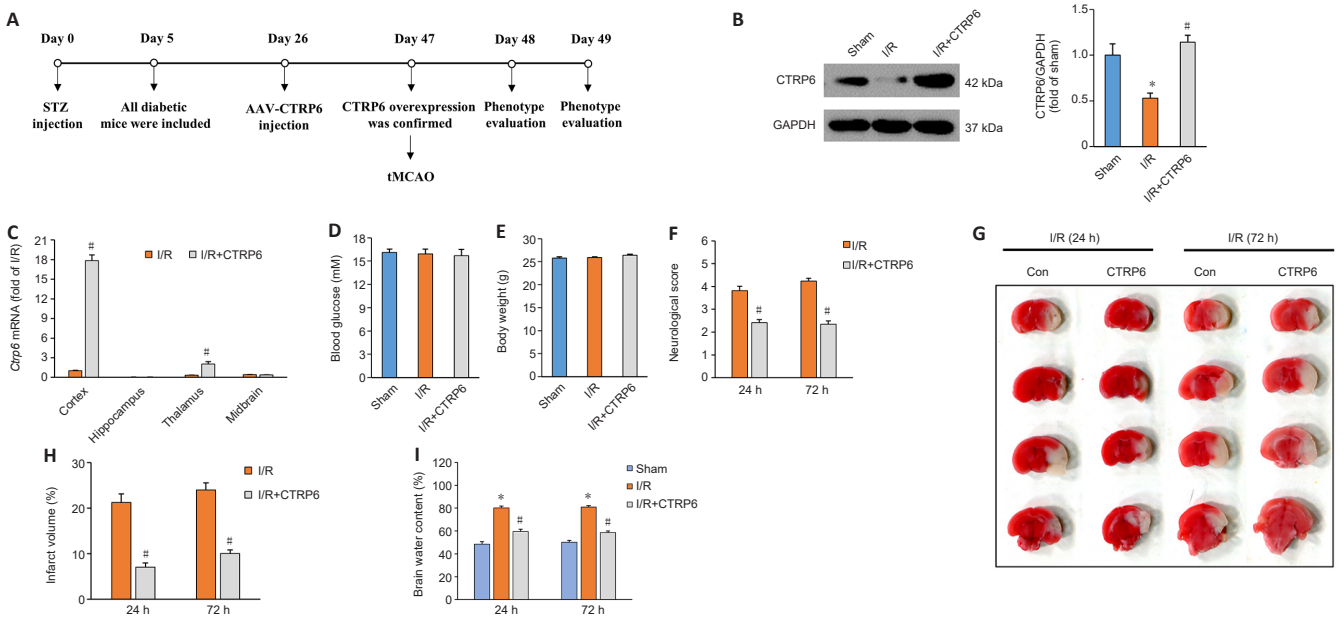

Figure 3 | C1q/tumor necrosis factor-related protein-6 (CTRP6) overexpression attenuates cerebral ischemia/reperfusion (I/R) injury in diabetic mice.
(A) The timeline of experimental procedures. To overexpress cerebral CTRP6, mice from the I/R + CTRP6 group received an injection of adeno-associated virus-2/9 (AAV-2/9) carrying human CTRP6 (AAV-CTRP6) 3 weeks after streptozotocin (STZ) injection. Mice in the Sham and I/R groups received AAV-negative control (NC) injection. (B) CTRP6 protein expression in the three groups after I/R or Sham I/R (six animals per group). (C) *Ctrp6* mRNA expression in different regions of the brain after AAV-CTRP6 or sham infection (three to five animals per group). (D, E) Blood glucose and body weight in mice overexpressing CTRP6 24 hours after I/R (eight animals per group). (F) Neurological scores in mice following I/R (eight animals per group, 24 hours after I/R; nine animals per group, 72 hours after I/R). (G–I) Infarct volume (G, H) and brain water content (I) in diabetic mice (eight animals per group, 24 hours after I/R; nine animals per group, 72 hours after I/R). White regions show infarct areas in G. All data were normalized to the Sham or I/R groups. Results are presented as the mean ± SEM, and were analyzed by unpaired two-sided Student's *t*-test (E and G) or one-way analysis of variance followed by *post hoc* Tukey's test (B–D and H). *$P < 0.05$, *vs.* Sham group; #$P < 0.05$, *vs.* I/R group. GAPDH: Glyceraldehyde-3-phosphate dehydrogenase; tMCAO: transient middle cerebral artery occlusion.

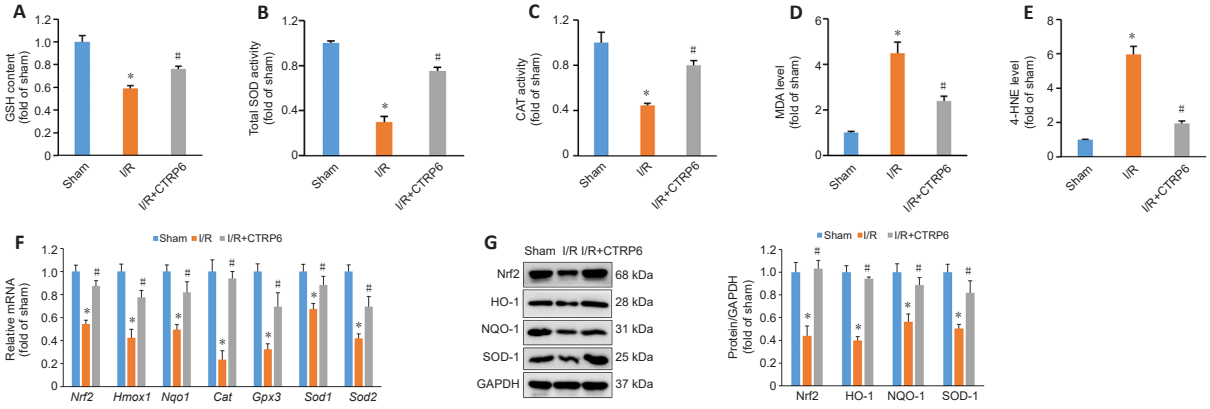

Figure 4 | **C1q/tumor necrosis factor-related protein-6 (CTRP6) overexpression prevents ischemia/reperfusion (I/R)-induced oxidative stress in the brain.**
(A–E) Glutathione (GSH) content (A), total superoxide dismutase (SOD) activity (B), catalase (CAT) activity (C), malondialdehyde (MDA) content (D) and 4-hydroxynonenal (4-HNE) levels (E) were measured to estimate oxidative damage caused by 24-hour I/R (six animals per group). (F, G) Nuclear factor (erythroid-2 related) factor 2 (Nrf2) and its downstream target gene levels (F) and protein expression (G) (six animals per group). All data were normalized to the Sham group. The results are presented as the mean ± SEM, and were analyzed by one-way analysis of variance followed by *post hoc* Tukey's test. *P < 0.05, *vs*. Sham group; #P < 0.05, *vs*. I/R group. GAPDH: Glyceraldehyde-3-phosphate dehydrogenase.

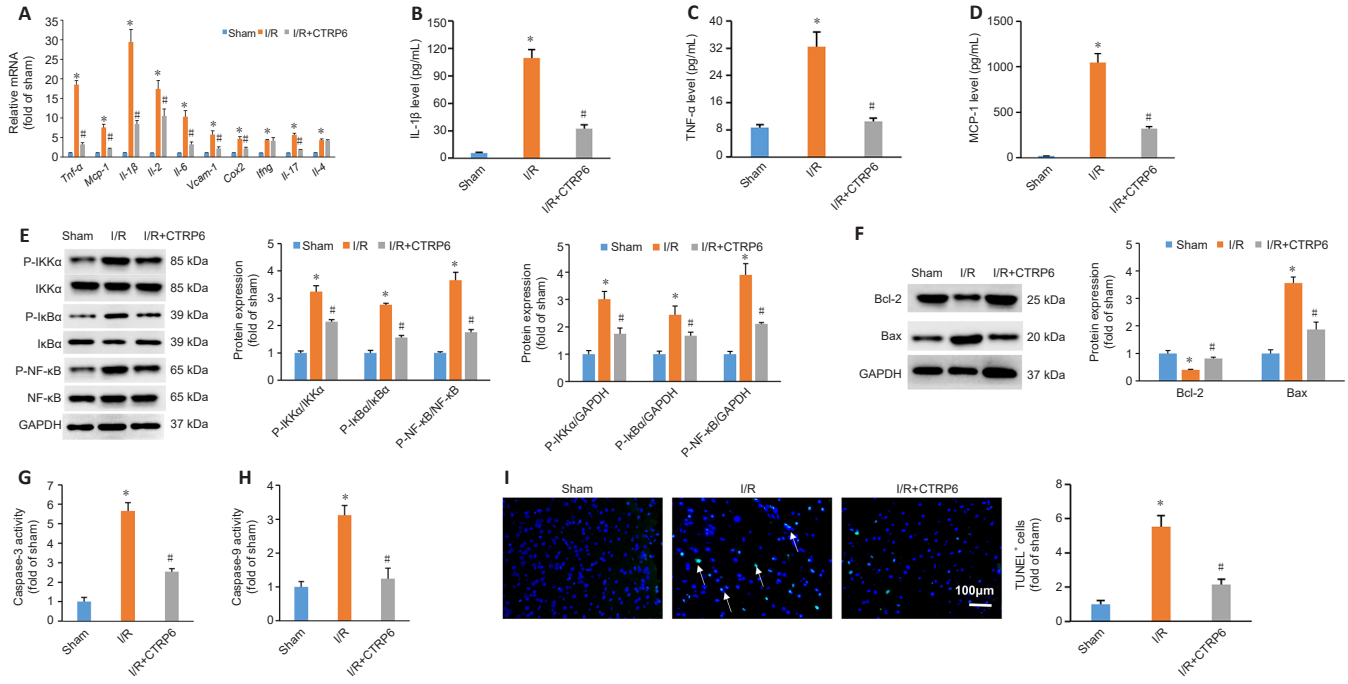

Figure 5 | **C1q/tumor necrosis factor-related protein-6 (CTRP6) overexpression attenuates ischemia/reperfusion (I/R)-induced inflammatory responses and apoptosis in the brain.**
(A–D) mRNA levels of inflammatory factors (A), interleukin-1β (IL-1β) protein level (B), tumor necrosis factor-α (TNF-α) protein level (C), and monocyte chemoattractant protein-1 (MCP-1) protein level (D) were measured to estimate inflammatory responses caused by 24-hour I/R (six animals per group). (E) Nuclear factor kappa B (NF-κB) signaling pathway (six animals per group). (F) Protein expression levels of Bcl-2 and Bax (six animals per group). (G, H) Caspase-3 and caspase-9 activity (six animals per group). (I) TUNEL staining in the brain (six animals per group). Blue is positive signal as indicated in the I/R group. Scale bar: 100 μm. All data were normalized to the Sham group. The results are presented as the mean ± SEM, and were analyzed by one-way analysis of variance followed by *post hoc* Tukey's test. *P < 0.05, *vs*. Sham group; #P < 0.05, *vs*. I/R group. GAPDH: Glyceraldehyde-3-phosphate dehydrogenase; TUNEL: terminal deoxynucleotidyl transferase-mediated dUTP nick end labeling.

Nqo1, *Cat*, *Gpx3*, *Sod1*, and *Sod2* were significantly reduced in response to H/R stimuli in high glucose-pretreated cortical neurons, and these declines were prevented by CTRP6 (**Figure 6F**). Similarly, Nrf2 and HO-1 expression were downregulated in high glucose-pretreated cells after exposure to H/R, and these declines were prevented by CTRP6 (**Figure 6G**). Next, we assessed whether CTRP6 affected Nrf2 transcriptional activity. A reduction in Nrf2 transcriptional activity was observed in high glucose-pretreated cells after exposure to H/R, and CTRP6 overexpression largely improved Nrf2 transcriptional activity (**Figure 6H**). CTRP6 overexpression also significantly suppressed ROS and 4-HNE production in cells after exposure to H/R (**Figure 6I** and **J**). A luciferase assay also suggested that CTRP6 overexpression largely decreased NF-κB transcriptional activity in these H/R-treated neurons (**Figure 6K**). Further analysis showed that CTRP6 overexpression suppressed all inflammatory mediators, except Ifng (**Figure 6L**). CTRP6 overexpression also attenuated TNF-α protein expression (**Figure 6M**); decreased NF-κB activity, as revealed by the alteration in the phosphorylation of NF-κB (**Figure 6N**); restored Bcl-2 protein expression (**Figure 6N**); and prevented the increase in caspase 3 activity observed in H/R-exposed cortical neurons (**Figure 6O**).

CTRP6 enhances the Sirt1 signaling pathway in mice after I/R injury

Sirt1 negatively regulates the NF-κB pathway and is involved in cerebral diseases (Yoon et al., 2015). Therefore, we asked whether CTRP6 activated Sirt1 to protect neurons from H/R injury. I/R significantly decreased cerebral Sirt1 protein expression, and this reduction was significantly prevented by CTRP6 treatment (**Figure 7A**). The decreased Sirt1 protein expression caused by H/R was also significantly restored in CTRP6-overexpressing neurons (**Figure 7B**). Next, a specific Sirt1 inhibitor (Ex527) was used. As expected, CTRP6 significantly increased cell viability and reduced LDH release in H/R-exposed neurons, and these benefits provided by CTRP6 were offset by the use of Ex527 (**Figure 7C** and **D**). Moreover, CTRP6 decreased the production of ROS and enhanced Nrf2 transcriptional activity in H/R-exposed neurons, and these effects were abolished by Sirt1 inhibition (**Figure 7E** and **F**). NF-κB transcriptional activity in H/R-treated neurons was also limited by CTRP6 overexpression, and this inhibitory effect of CTRP6 was offset by the Sirt1 inhibitor (**Figure 7G**). Ex527 also abrogated the inhibitory effects of CTRP6 on *Tnf-α* and caspase 3 activity in H/R-exposed neurons (**Figure 7H** and **I**).

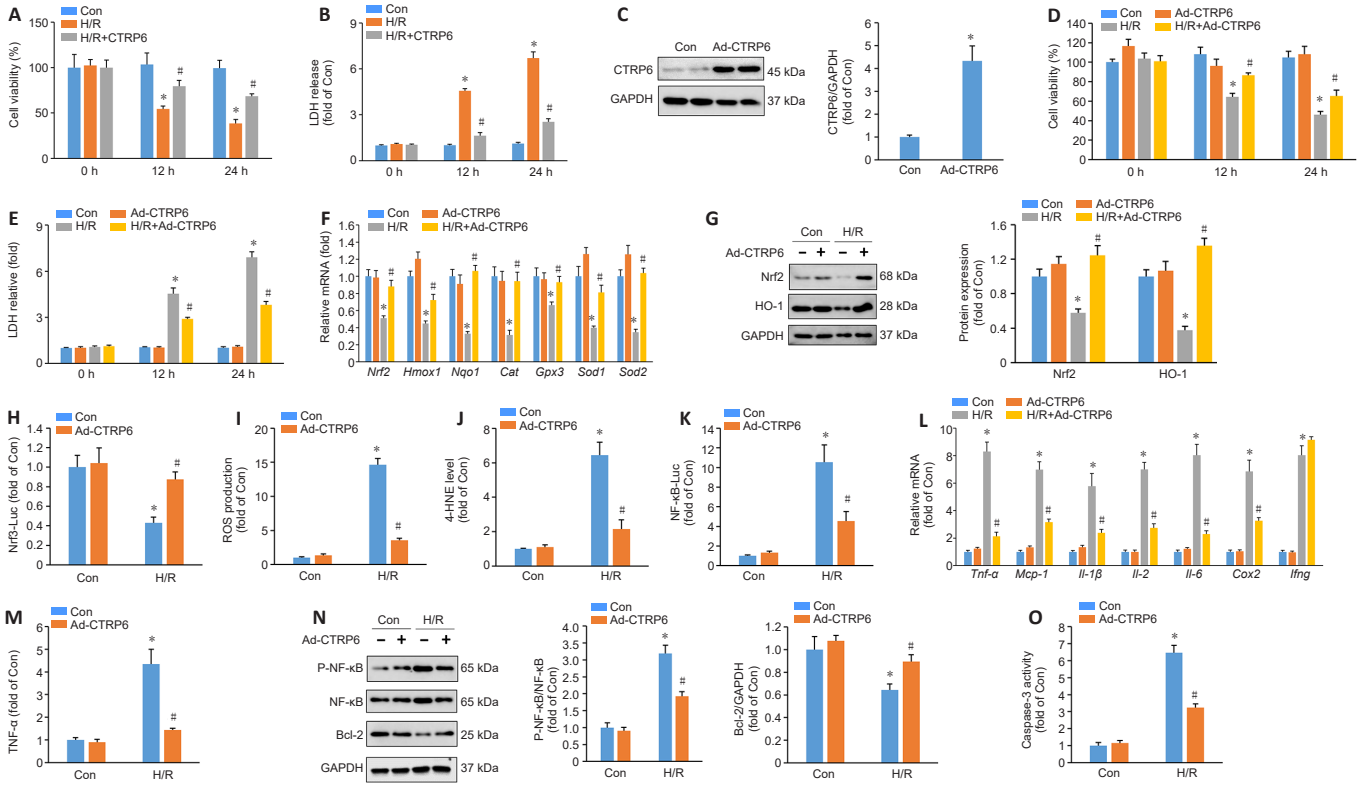

Figure 6 | **C1q/tumor necrosis factor-related protein-6 (CTRP6) protects cortical neurons from hypoxia/reoxygenation (H/R) *in vitro*.**
(A, B) Viability of cortical neurons and lactate dehydrogenase (LDH) release after CTRP6 treatment. (C) CTRP6 protein expression after adenoviral vectors carrying CTRP6 (Ad-CTRP6) infection. (D, E) Cell viability and LDH release after CTRP6 overexpression. (F) The mRNA levels of Nrf2 and *Nrf2*-regulated genes. (G) The protein expression of Nrf2 and Nrf2-regulated targets. (H) Nrf2 transcriptional activity. (I, J) The production of reactive oxygen species (ROS) and 4-hydroxynonenal (4-HNE) after CTRP6 overexpression. (K) Nuclear factor kappa B (NF-κB) transcriptional activity. (L) The mRNA levels of NF-κB-regulated genes. (M) Tumor necrosis factor-α (TNF-α) protein level. (N) The protein expression of NF-κB and Bcl-2 after CTRP6 overexpression. (O) Caspase-3 activity after CTRP6 overexpression. For (A), five independent cortical neuron preparations per group at each time point; for others, five or six independent cortical neuron preparations per group. All data were normalized to the control group. The results are presented as the mean ± SEM, and were analyzed by unpaired two-sided Student's *t*-test (C) or one-way analysis of variance followed by *post hoc* Tukey's test (others). *$P < 0.05$, *vs.* control (Con) group; #$P < 0.05$, *vs.* H/R group. GAPDH: glyceraldehyde-3-phosphate dehydrogenase; IL: interleukin; Mcp-1: monocyte chemoattractant protein-1; P-NF-κB: phosphorylated-NF-κB; Tnf-α: tumor necrosis factor-α.

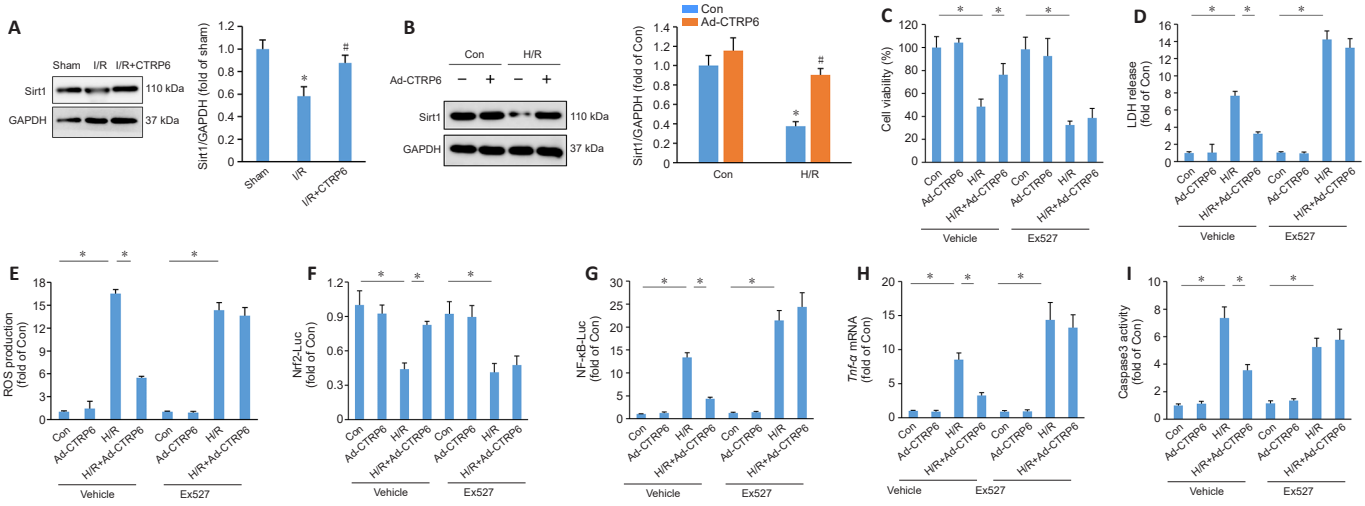

Figure 7 | **C1q/tumor necrosis factor-related protein-6 (CTRP6) protects against hypoxia/reoxygenation (H/R)-induced inflammation and oxidative damage via the sirtuin 1 (Sirt1) signaling pathway *in vitro*.**
(A, B) Sirt1 protein expression after CTRP6 treatment. *$P < 0.05$, *vs.* Sham group or control (Con) group; #$P < 0.05$, *vs.* I/R or H/R group. (C, D) Cell viability and lactate dehydrogenase (LDH) release after Ex527 treatment. (E, F) Reactive oxygen species (ROS) production and nuclear factor (erythroid-2 related) factor 2 (Nrf2) transcriptional activity after Ex527 treatment. (G, H) Nuclear factor kappa B (NF-κB) transcriptional activity and *Tnf-α* mRNA level. (I) Caspase 3 activity after Ex527 treatment. For each experiment, six independent cortical neuron preparations were made per group. All data were normalized to the sham, control (Con), or Ad-control group. The results are presented as the mean ± SEM, and were analyzed by one-way analysis of variance followed by *post hoc* Tukey's test. For C–F, *$P < 0.05$, *vs.* Con group. Ex527: A specific inhibitor of Sirt1; GAPDH: glyceraldehyde-3-phosphate dehydrogenase; I/R: ischemia/reperfusion; Tnf-α: tumor necrosis factor-α.

CTRP6 no longer protects against cerebral I/R injury in *Sirt1*-deficient diabetic mice

Next, we used mice with neuron-specific depletion of *Sirt1* (**Figure 8A**). CTRP6 supplementation in the absence of *Sirt1* could not provide protection against I/R-induced injury, as reflected by infarct volume and neurological deficits (**Figure 8B** and **C**). The inhibitory effects of CTRP6 on MDA production were also blocked by *Sirt1* deficiency (**Figure 8D**). In *Sirt1*-deficient mice, CTRP6 did not increase total SOD activity in the model mice following focal cerebral I/R (**Figure 8E**). Further analysis of anti-oxidative gene expression confirmed that the inhibitory effects of CTRP6 were blocked by *Sirt1* deficiency (**Figure 8F**). The decreased nuclear NF-κB and inflammatory factors after CTRP6 treatment were also abolished by *Sirt1* knockout (**Figure 8G** and **H**). *Sirt1* knockout also abrogated the anti-apoptotic effects of CTRP6 in the model mice following focal cerebral I/R (**Figure 8I**).

CTRP6 activates Sirt1 via a nicotinamide adenine dinucleotide (NAD)$^+$-dependent manner

We found that, as expected, CTRP6 supplementation led to higher NAD^+ levels and higher NAD^+/NADH ratios in the brains, both of which were reduced by I/R or H/R in the model mice.

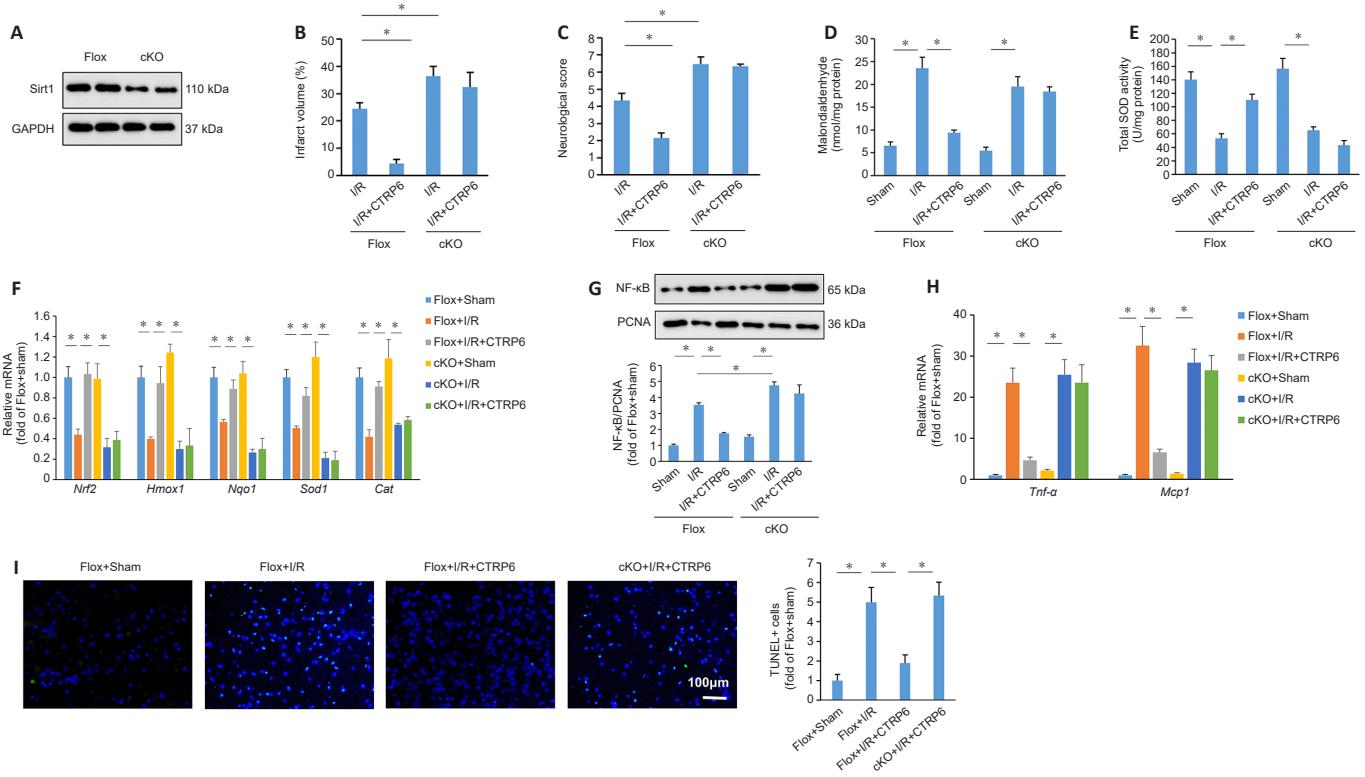

Figure 8 | **C1q/tumor necrosis factor-related protein-6 (CTRP6) cannot protect against ischemia/reperfusion (I/R) injury in sirtuin 1 (Sirt1)-deficient mice.**
(A) Sirt1 protein expression after CTRP6 treatment (six animals per group). (B, C) Infarct volume and neurological score in mice following I/R (10 animals per group). (D, E) Malondialdehyde (MDA) content and total superoxide dismutase (SOD) activity in mice following 24-hour I/R (six animals per group). (F) The mRNA levels for *Nrf2* and Nrf2-regulated genes (six animals per group). (G) Protein expression of nuclear factor kappa B (NF-κB) (six animals per group). (H) The mRNA levels for *Tnf-α* and *Mcp-1* (six animals per group). (I) TUNEL staining in the brain (six animals per group). All data were normalized to the Flox + sham group. Results are presented as the mean ± SEM. These data were analyzed by unpaired two-sided Student's *t*-test (A) and one-way analysis of variance followed by *post hoc* Tukey's test (others). **P* < 0.05, *vs.* Flox + sham group. Cat: Catalase; cKO: CTRP6 knockout; GAPDH: glyceraldehyde-3-phosphate dehydrogenase; Nrf2: nuclear factor (erythroid-2 related) factor 2; PCNA: proliferating cell nuclear antigen; Sod: superoxide dismutase; Tnf-α: tumor necrosis factor-α; TUNEL: terminal deoxynucleotidyl transferase-mediated dUTP nick end labeling.

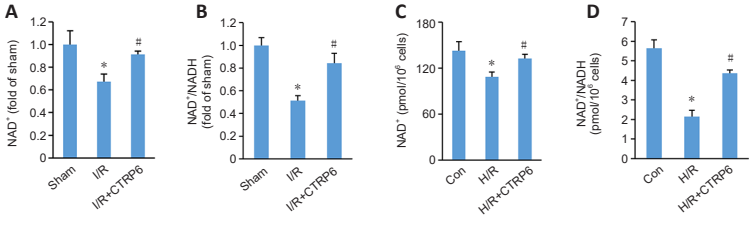

Figure 9 | **CTRP6 increases nicotinamide adenine dinucleotide (NAD)$^+$ and the NAD$^+$/ reduced NAD (NADH) ratio *in vivo* and *in vitro*.**
(A, B) NAD$^+$ and NAD$^+$/NADH ratio after CTRP6 treatment *in vivo* (six animals per group). (C, D) NAD$^+$ and the NAD$^+$/NADH ratio after CTRP6 treatment *in vitro* (six independent cortical neurons preparations per group). All data were normalized to the sham or control (Con) group. The results are presented as the mean ± SEM, and were analyzed by one-way analysis of variance followed by *post hoc* Tukey's test. **P* < 0.05, *vs.* Sham (Con) group; #*P* < 0.05, *vs.* ischemia/reperfusion (I/R) or hypoxia/reoxygenation (H/R) group.

Discussion

Our results show that CTRP6 deficiency in neurons caused the accumulation of ROS and inflammatory factors and led to cell death. CTRP6 overexpression suppressed cerebral I/R injury, redox imbalance, and cerebral death in the model diabetic mice. The neuroprotection afforded by CTRP6 depended on activation of Sirt1, and thus *Sirt1* knockout eliminated the protection *in vivo*. Our findings suggest that CTRP6 is a novel therapeutic target for treating diabetic stroke.

Several studies have indicated the involvement of CTRP6 in cardio-metabolic diseases. Circulating CTRP6 levels were upregulated in obese patients and positively correlated with body mass index (Liao et al., 2021). Wang et al. (2018b) found that CTRP6 can promote the progression of diabetes. In contrast, Lahav et al. (2021) reported that CTRP6 can rapidly respond to acute stimuli and inhibit adipose tissue expansion. Our results showed that CTRP6 levels in diabetic brains were downregulated following cerebral I/R. CTRP6 deficiency even without H/R stimuli could cause redox imbalance, inflammation, and apoptosis, recapitulating the phenotype of I/R-induced brain injury. Therefore, we asked whether optimizing CTRP6 levels in diabetic brains would alleviate cerebral I/R injury. As expected, CTRP6 overexpression could alleviate I/R-related cerebral injury in diabetic mice, indicating that CTRP6 is a promising target for the treatment of cerebral I/R injury in patients with diabetes.

Oxidative stress has been reported to participate in regulating the development of diabetic stroke (Su et al., 2020). Free radicals caused by I/R exert profoundly harmful effects on neurons and activate apoptosis-related pathways (Orellana-Urzúa et al., 2020). Here, we found that I/R-induced cerebral oxidative damage was mitigated by CTRP6 overexpression. Oxidative stress is the consequence of an imbalance between pro- and anti-oxidant systems. Nrf2 is a well-known and important transcription factor that is responsible for transcription of some antioxidant genes (Liao et al., 2020). CTRP6 increased Nrf2 levels and those of its downstream targets, which indicates that CTRP6 might inhibit I/R-related oxidative stress via upregulation of an anti-oxidant.

Inflammation has also been reported to be involved in ischemic stroke (Anrather and Iadecola, 2016; Li et al., 2020a), especially in cases of diabetes. Injured neurons in diabetic mice activate glial cells and recruit leukocytes to secrete cytokine, forming a pro-inflammatory microenvironment and exacerbating tissue injury (Li et al., 2020b). Here, we found that CTRP6 overexpression largely reduced cerebral inflammation in mice subjected to I/R exposure. Moreover, protein expression and activation of NF-κB were also suppressed in the ischemic brains of diabetic mice after the overexpression of CTRP6. Interestingly, we also found that CTRP6 deficiency promoted NF-κB activation and onset of inflammation *in vitro*, even in the absence of H/R. However, in stark contrast, another study has reported that CTRP6 increased TNF-α expression (Wang et al., 2018a). This inconsistency might be attributed to the different roles of CTRP6 in different tissues and different diseases.

Apoptosis is another critical mediator of diabetic stroke (Broughton et al., 2009). Apoptosis begins several minutes after ischemic onset (Broughton et al., 2009). Moreover, inhibition of neuronal apoptosis can prevent ischemic injury in diabetic mice (Gong et al., 2017). CTRP6 has been reported to attenuate loss of salivary acinar cells (Qu et al., 2021) and apoptosis of PC12 cells *in vitro* (Li et al., 2020b). More recently, CTRP6 was shown to attenuate DOX-induced myocardial apoptosis in mice (Zheng et al., 2019). In the current study, we also found that CTRP6 plays an anti-apoptotic role in I/R-related cerebral injury. CTRP6 supplementation significantly decreased the number of apoptotic cells and the amount of caspase 3 activity after cerebral ischemia.

Sirt1 is involved in neuroprotection (Meng et al., 2017). Sirt1 activation can protect against ischemic stroke by upregulating peroxisome proliferator-

activated receptor alpha (PPARα) signaling pathways (Shin et al., 2012). In our study, restoration of Sirt1 expression by overexpression of CTRP6 attenuated the I/R-related pathology in diabetic mice. More importantly, Sirt1 loss of function abrogated the neuroprotection provided by CTRP6, suggesting that the neuroprotection afforded by CTRP6 can be attributed to Sirt1 activation. As reported, Sirt1 is an NAD^+-dependent deacetylase. We also found that CTRP6 increased NAD^+ and the NAD^+/NADH ratio in diabetic mice after cerebral ischemia, indicating that CTRP6 might activate Sirt1 in an NAD^+-dependent manner.

Our study also has some limitations. We only used male mice to investigate the role of CTRP6 in diabetic stroke. We did not confirm the expression and the key role of CTRP6 in other large animals. In conclusion, we found CTRP6 acted to protect the mouse brain from diabetic stroke by inhibiting neuronal apoptosis, inflammatory mediator release, and oxidative damage. CTRP6 might be a promising therapeutic target for treating ischemic stroke, especially in patients with diabetes.

Author contributions: *Study conception and design: BZ, WG and LG. Study implementation and data acquisition: BZ, ML, BL, and YL. Data analysis and interpretation: BZ, ML, QS, JH, and YW. Manuscript writing and revision: BZ, WG, and LG. Guarantors: WG and LG. All authors approved the final version of the manuscript.*

Conflicts of interest: *The authors declare that they have no competing interests.*

Data availability statement: *All relevant data are within the paper.*

Open peer reviewer: *Maya Maor-Nof, Stanford University, USA.*

Additional file: *Open peer review report 1.*

References

Allen CL, Bayraktutan U (2009) Oxidative stress and its role in the pathogenesis of ischaemic stroke. Int J Stroke 4:461-470.

Alloubani A, Saleh A, Abdelhafiz I (2018) Hypertension and diabetes mellitus as a predictive risk factors for stroke. Diabetes Metab Syndr 12:577-584.

Anrather J, Iadecola C (2016) Inflammation and stroke: an overview. Neurotherapeutics 13:661-670.

Broughton BR, Reutens DC, Sobey CG (2009) Apoptotic mechanisms after cerebral ischemia. Stroke 40:e331-339.

Capes SE, Hunt D, Malmberg K, Pathak P, Gerstein HC (2001) Stress hyperglycemia and prognosis of stroke in nondiabetic and diabetic patients: a systematic overview. Stroke 32:2426-2432.

Chen J, Ye X, Yan T, Zhang C, Yang XP, Cui X, Cui Y, Zacharek A, Roberts C, Liu X, Dai X, Lu M, Chopp M (2011) Adverse effects of bone marrow stromal cell treatment of stroke in diabetic rats. Stroke 42:3551-3558.

Desilles JP, Meseguer E, Labreuche J, Lapergue B, Sirimarco G, Gonzalez-Valcarcel J, Lavallée P, Cabrejo L, Guidoux C, Klein I, Amarenco P, Mazighi M (2013) Diabetes mellitus, admission glucose, and outcomes after stroke thrombolysis: a registry and systematic review. Stroke 44:1915-1923.

Fang XX, Xu FF, Liu Z, Cao BB, Qiu YH, Peng YP (2022) Interleukin 17A deficiency alleviates neuroinflammation and cognitive impairment in an experimental model of diabetic encephalopathy. Neural Regen Res 17:2771-2777.

Forrester SJ, Kikuchi DS, Hernandes MS, Xu Q, Griendling KK (2018) Reactive oxygen species in metabolic and inflammatory signaling. Circ Res 122:877-902.

Gong L, Tang Y, An R, Lin M, Chen L, Du J (2017) RTN1-C mediates cerebral ischemia/reperfusion injury via ER stress and mitochondria-associated apoptosis pathways. Cell Death Dis 8:e3080.

Gray SJ, Woodard KT, Samulski RJ (2010) Viral vectors and delivery strategies for CNS gene therapy. Ther Deliv 1:517-534.

Gu L, Xiong X, Zhang H, Xu B, Steinberg GK, Zhao H (2012) Distinctive effects of T cell subsets in neuronal injury induced by cocultured splenocytes in vitro and by in vivo stroke in mice. Stroke 43:1941-1946.

Lahav R, Haim Y, Bhandarkar NS, Levin L, Chalifa-Caspi V, Sarver D, Sahagun A, Maixner N, Kovesh B, Wong GW, Rudich A (2021) CTRP6 rapidly responds to acute nutritional changes, regulating adipose tissue expansion and inflammation in mice. Am J Physiol Endocrinol Metab 321:E702-E713.

Lei X, Seldin MM, Little HC, Choy N, Klonisch T, Wong GW (2017) C1q/TNF-related protein 6 (CTRP6) links obesity to adipose tissue inflammation and insulin resistance. J Biol Chem 292:14836-14850.

Li Q, Cao Y, Dang C, Han B, Han R, Ma H, Hao J, Wang L (2020a) Inhibition of double-strand DNA-sensing cGAS ameliorates brain injury after ischemic stroke. EMBO Mol Med 12:e11002.

Li Y, Sun J, Gu L, Gao X (2020b) Protective effect of CTRP6 on cerebral ischemia/reperfusion injury by attenuating inflammation, oxidative stress and apoptosis in PC12 cells. Mol Med Rep 22:344-352.

Liao S, Wu J, Liu R, Wang S, Luo J, Yang Y, Qin Y, Li T, Zheng X, Song J, Zhao X, Xiao C, Zhang Y, Bian L, Jia P, Bai Y, Zheng X (2020) A novel compound DBZ ameliorates neuroinflammation in LPS-stimulated microglia and ischemic stroke rats: Role of Akt(Ser473)/GSK3β(Ser9)-mediated Nrf2 activation. Redox Biol 36:101644.

Liao X, Liu S, Tang X, Yang D, Liu H, Gao L, Yang G (2021) Circulating CTRP6 levels are increased in overweight or obese Chinese Individuals and associated with insulin resistance parameters: a pilot study. Exp Clin Endocrinol Diabetes 129:535-541.

Lindsberg PJ, Grau AJ (2003) Inflammation and infections as risk factors for ischemic stroke. Stroke 34:2518-2532.

Liu L, Cao Q, Gao W, Li B, Xia Z, Zhao B (2021) Melatonin protects against focal cerebral ischemia-reperfusion injury in diabetic mice by ameliorating mitochondrial impairments: involvement of the Akt-SIRT3-SOD2 signaling pathway. Aging (Albany NY) 13:16105-16123.

Liu P, Zhao H, Wang R, Wang P, Tao Z, Gao L, Yan F, Liu X, Yu S, Ji X, Luo Y (2015) MicroRNA-424 protects against focal cerebral ischemia and reperfusion injury in mice by suppressing oxidative stress. Stroke 46:513-519.

Lu YY, Li ZZ, Jiang DS, Wang L, Zhang Y, Chen K, Zhang XF, Liu Y, Fan GC, Chen Y, Yang Q, Zhou Y, Zhang XD, Liu DP, Li H (2013) TRAF1 is a critical regulator of cerebral ischaemia-reperfusion injury and neuronal death. Nat Commun 4:2852.

Ma ZG, Dai J, Zhang WB, Yuan Y, Liao HH, Zhang N, Bian ZY, Tang QZ (2016) Protection against cardiac hypertrophy by geniposide involves the GLP-1 receptor / AMPKα signalling pathway. Br J Pharmacol 173:1502-1516.

Ma ZG, Yuan YP, Xu SC, Wei WY, Xu CR, Zhang X, Wu QQ, Liao HH, Ni J, Tang QZ (2017) CTRP3 attenuates cardiac dysfunction, inflammation, oxidative stress and cell death in diabetic cardiomyopathy in rats. Diabetologia 60:1126-1137.

Meng X, Tan J, Li M, Song S, Miao Y, Zhang Q (2017) Sirt1: role under the condition of ischemia/hypoxia. Cell Mol Neurobiol 37:17-28.

Morgan MJ, Liu ZG (2011) Crosstalk of reactive oxygen species and NF-κB signaling. Cell Res 21:103-115.

Moro MA, Almeida A, Bolaños JP, Lizasoain I (2005) Mitochondrial respiratory chain and free radical generation in stroke. Free Radic Biol Med 39:1291-1304.

NIH Office of Animal Care and Use (2021) Guidelines for Euthanasia of Rodent Fetuses and Neonates. https://oacu.oir.nih.gov/system/files/media/file/2021-02/b4_rodent_euthanasia_pup.pdf. Accessed December 27, 2022.

Orellana-Urzúa S, Rojas I, Líbano L, Rodrigo R (2020) Pathophysiology of ischemic stroke: role of oxidative stress. Curr Pharm Des 26:4246-4260.

Pacher P, Haskó G (2008) Endocannabinoids and cannabinoid receptors in ischaemia-reperfusion injury and preconditioning. Br J Pharmacol 153:252-262.

Percie du Sert N, Hurst V, Ahluwalia A, Alam S, Avey MT, Baker M, Browne WJ, Clark A, Cuthill IC, Dirnagl U, Emerson M, Garner P, Holgate ST, Howells DW, Karp NA, Lazic SE, Lidster K, MacCallum CJ, Macleod M, Pearl EJ, et al. (2020) The ARRIVE guidelines 2.0: Updated guidelines for reporting animal research. PLoS Biol 18:e3000410.

Qiu J, Guo J, Liu L, Liu X, Sun X, Chen H (2023) Vav1 promotes inflammation and neuronal apoptosis in cerebral ischemia/reperfusion injury by upregulating microglial and NLRP3 inflammasome activation. Neural Regen Res 18:2436-2442.

Qu LH, Hong X, Zhang Y, Cong X, Xiang RL, Mei M, Su JZ, Wu LL, Yu GY (2021) C1q/tumor necrosis factor-related protein-6 attenuates TNF-α-induced apoptosis in salivary acinar cells via AMPK/SIRT1-modulated miR-34a-5p expression. J Cell Physiol 236:5785-5800.

Shin JA, Lee KE, Kim HS, Park EM (2012) Acute resveratrol treatment modulates multiple signaling pathways in the ischemic brain. Neurochem Res 37:2686-2696.

Stoll G, Nieswandt B (2019) Thrombo-inflammation in acute ischaemic stroke-implications for treatment. Nat Rev Neurol 15:473-481.

Su XT, Wang L, Ma SM, Cao Y, Yang NN, Lin LL, Fisher M, Yang JW, Liu CZ (2020) Mechanisms of acupuncture in the regulation of oxidative stress in treating ischemic stroke. Oxid Med Cell Longev 2020:7875396.

Ugidos IF, González-Rodríguez P, Santos-Galdiano M, Font-Belmonte E, Anuncibay-Soto B, Pérez-Rodríguez D, Gonzalo-Orden JM, Fernández-López A (2023) Neuroprotective effects of meloxicam on transient brain ischemia in rats: the two faces of anti-inflammatory treatments. Neural Regen Res 18:1961-1967.

Wang L, Lu Y, Deng S, Zhang Y, Yang L, Guan Y, Matozaki T, Ohnishi H, Jiang H, Li H (2012) SHPS-1 deficiency induces robust neuroprotection against experimental stroke by attenuating oxidative stress. J Neurochem 122:834-843.

Wang L, Lu Y, Guan H, Jiang D, Guan Y, Zhang X, Nakano H, Zhou Y, Zhang Y, Yang L, Li H (2013) Tumor necrosis factor receptor-associated factor 5 is an essential mediator of ischemic brain infarction. J Neurochem 126:400-414.

Wang M, Tang X, Li L, Liu D, Liu H, Zheng H, Deng W, Zhao X, Yang G (2018a) C1q/TNF-related protein-6 is associated with insulin resistance and the development of diabetes in Chinese population. Acta Diabetol 55:1221-1229.

Wang S, Sun Z, Yang S, Chen B, Shi J (2018b) CTRP6 inhibits cell proliferation and ECM expression in rat mesangial cells cultured under TGF-β1. Biomed Pharmacother 97:280-285.

Wang Y, Hu H, Yin J, Shi Y, Tan J, Zheng L, Wang C, Li X, Xue M, Liu J, Wang Y, Li Y, Li X, Liu F, Liu Q, Yan S (2019) TLR4 participates in sympathetic hyperactivity Post-MI in the PVN by regulating NF-κB pathway and ROS production. Redox Biol 24:101186.

Wu W, Zhang J, Zhao C, Sun Y, Yin Y, Peng Y, Pang W, Yang G (2018) Lentivirus-mediated CTRP6 silencing ameliorates diet-induced obesity in mice. Exp Cell Res 367:15-23.

Xiang H, Xue W, Li Y, Zheng J, Ding C, Dou M, Wu X (2020) C1q/TNF-related protein 6 (CTRP6) attenuates renal ischaemia-reperfusion injury through the activation of PI3K/Akt signalling pathway. Clin Exp Pharmacol Physiol 47:1030-1040.

Xiong XX, Gu LJ, Shen J, Kang XH, Zheng YY, Yue SB, Zhu SM (2014) Probenecid protects against transient focal cerebral ischemic injury by inhibiting HMGB1 release and attenuating AQP4 expression in mice. Neurochem Res 39:216-224.

Yoon MJ, Yoshida M, Johnson S, Takikawa A, Usui I, Tobe K, Nakagawa T, Yoshino J, Imai S (2015) SIRT1-mediated eNAMPT secretion from adipose tissue regulates hypothalamic NAD+ and function in mice. Cell Metab 21:706-717.

Zheng WF, Zhang SY, Ma HF, Chang XW, Wang H (2019) C1qTNF-related protein-6 protects against doxorubicin-induced cardiac injury. J Cell Biochem 120:10748-10755.

C-Editor: Zhao M; S-Editors: Yu J, Li CH; L-Editors: Phillips A, Song LP; T-Editor: Jia Y